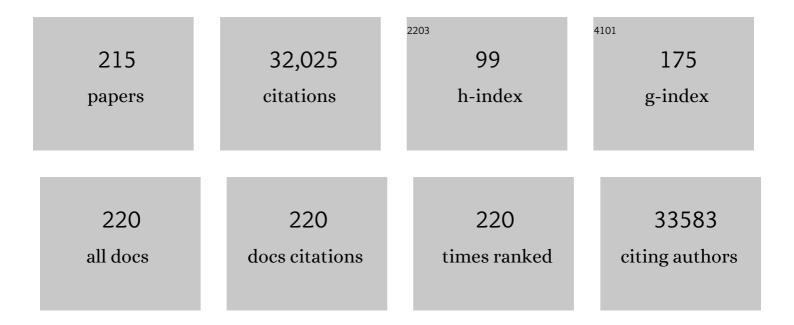
List of Publications by Year in descending order

Source: https://exaly.com/author-pdf/8581902/publications.pdf Version: 2024-02-01



Γιάνο Υλν

#	Article	IF	CITATIONS
1	Toxicity of manufactured nanomaterials. Particuology, 2022, 69, 31-48.	2.0	63
2	Orally administered Bi2S3@SiO2 core-shell nanomaterials as gastrointestinal contrast agents and their influence on gut microbiota. Materials Today Bio, 2022, 13, 100178.	2.6	5
3	Combinational application of metal–organic frameworksâ€based nanozyme and nucleic acid delivery in cancer therapy. Wiley Interdisciplinary Reviews: Nanomedicine and Nanobiotechnology, 2022, 14, e1773.	3.3	16
4	A Photosensitizer Discretely Loaded Nanoaggregate with Robust Photodynamic Effect for Local Treatment Triggers Systemic Antitumor Responses. ACS Nano, 2022, 16, 3070-3080.	7.3	38
5	Transformable Galliumâ€Based Liquid Metal Nanoparticles for Tumor Radiotherapy Sensitization. Advanced Healthcare Materials, 2022, 11, e2102584.	3.9	19
6	Effects of the Surface Charge of Graphene Oxide Derivatives on Ocular Compatibility. Nanomaterials, 2022, 12, 735.	1.9	0
7	A Copper Peroxide Fenton Nanoagent-Hydrogel as an <i>In Situ</i> pH-Responsive Wound Dressing for Effectively Trapping and Eliminating Bacteria. ACS Applied Bio Materials, 2022, 5, 1779-1793.	2.3	16
8	Precision design of engineered nanomaterials to guide immune systems for disease treatment. Matter, 2022, 5, 1162-1191.	5.0	11
9	Research trends in biomedical applications of two-dimensional nanomaterials over the last decade – A bibliometric analysis. Advanced Drug Delivery Reviews, 2022, 188, 114420.	6.6	25
10	Fractionated regimen-suitable immunoradiotherapy sensitizer based on ultrasmall Fe4Se2W18 nanoclusters enable tumor-specific radiosensitization augment and antitumor immunity boost. Nano Today, 2021, 36, 101003.	6.2	26
11	Nanomedicine enables spatiotemporally regulating macrophage-based cancer immunotherapy. Biomaterials, 2021, 268, 120552.	5.7	23
12	A pH-responsive ultrathin Cu-based nanoplatform for specific photothermal and chemodynamic synergistic therapy. Chemical Science, 2021, 12, 2594-2603.	3.7	78
13	The age of bioinspired molybdenumâ€involved nanozymes: Synthesis, catalytic mechanisms, and biomedical applications. View, 2021, 2, 20200188.	2.7	49
14	PEG-GO@XN nanocomposite suppresses breast cancer metastasis via inhibition of mitochondrial oxidative phosphorylation and blockade of epithelial-to-mesenchymal transition. European Journal of Pharmacology, 2021, 895, 173866.	1.7	11
15	X-ray-Based Techniques to Study the Nano–Bio Interface. ACS Nano, 2021, 15, 3754-3807.	7.3	60
16	A bibliometric analysis: Research progress and prospects on transition metal dichalcogenides in the biomedical field. Chinese Chemical Letters, 2021, 32, 3762-3770.	4.8	17
17	Photothermal Killing of A549 Cells and Autophagy Induction by Bismuth Selenide Particles. Materials, 2021, 14, 3373.	1.3	2
18	Highly Stable Silica-Coated Bismuth Nanoparticles Deliver Tumor Microenvironment-Responsive Prodrugs to Enhance Tumor-Specific Photoradiotherapy. Journal of the American Chemical Society, 2021, 143, 11449-11461.	6.6	51

#	Article	IF	CITATIONS
19	An overview of the use of nanozymes in antibacterial applications. Chemical Engineering Journal, 2021, 418, 129431.	6.6	140
20	X-ray-facilitated redox cycling of nanozyme possessing peroxidase-mimicking activity for reactive oxygen species-enhanced cancer therapy. Biomaterials, 2021, 276, 121023.	5.7	34
21	Plasmonic AuPt@CuS Heterostructure with Enhanced Synergistic Efficacy for Radiophotothermal Therapy. Journal of the American Chemical Society, 2021, 143, 16113-16127.	6.6	85
22	Rational Design of Nanomaterials for Various Radiationâ€Induced Diseases Prevention and Treatment. Advanced Healthcare Materials, 2021, 10, e2001615.	3.9	26
23	Reactive Oxygen Speciesâ€Regulating Strategies Based on Nanomaterials for Disease Treatment. Advanced Science, 2021, 8, 2002797.	5.6	149
24	Accelerated discovery of superoxide-dismutase nanozymes via high-throughput computational screening. Nature Communications, 2021, 12, 6866.	5.8	62
25	Layered double hydroxide nanosheets: towards ultrasensitive tumor microenvironment responsive synergistic therapy. Journal of Materials Chemistry B, 2020, 8, 1445-1455.	2.9	35
26	A Bi ₂ S ₃ @mSiO ₂ @Ag nanocomposite for enhanced CT visualization and antibacterial response in the gastrointestinal tract. Journal of Materials Chemistry B, 2020, 8, 666-676.	2.9	9
27	Two-dimensional nanomaterials beyond graphene for antibacterial applications: current progress and future perspectives. Theranostics, 2020, 10, 757-781.	4.6	152
28	Toxicological Evaluation of Graphene-Family Nanomaterials. Journal of Nanoscience and Nanotechnology, 2020, 20, 1993-2006.	0.9	46
29	Stimuli-Responsive Small-on-Large Nanoradiosensitizer for Enhanced Tumor Penetration and Radiotherapy Sensitization. ACS Nano, 2020, 14, 10001-10017.	7.3	93
30	Progress, challenges, and future of nanomedicine. Nano Today, 2020, 35, 101008.	6.2	135
31	Suppressing the Radiation-Induced Corrosion of Bismuth Nanoparticles for Enhanced Synergistic Cancer Radiophototherapy. ACS Nano, 2020, 14, 13016-13029.	7.3	42
32	Nano-bio interactions: the implication of size-dependent biological effects of nanomaterials. Science China Life Sciences, 2020, 63, 1168-1182.	2.3	58
33	Clinically Approved Carbon Nanoparticles with Oral Administration for Intestinal Radioprotection via Protecting the Small Intestinal Crypt Stem Cells and Maintaining the Balance of Intestinal Flora. Small, 2020, 16, e1906915.	5.2	51
34	Graphdiyne nanoradioprotector with efficient free radical scavenging ability for mitigating radiation-induced gastrointestinal tract damage. Biomaterials, 2020, 244, 119940.	5.7	58
35	Ultrasmall BiOI Quantum Dots with Efficient Renal Clearance for Enhanced Radiotherapy of Cancer. Advanced Science, 2020, 7, 1902561.	5.6	63
36	BiO _{2–<i>x</i>} Nanosheets as Radiosensitizers with Catalase-Like Activity for Hypoxia Alleviation and Enhancement of the Radiotherapy of Tumors. Inorganic Chemistry, 2020, 59, 3482-3493.	1.9	64

ARTICLE IF CITATIONS A Heterojunction Structured WO_{2.9}-WSe₂ Nanoradiosensitizer Increases Local Tumor Ablation and Checkpoint Blockade Immunotherapy upon Low Radiation Dose. ACS Nano, 104 2020, 14, 5400-5416. 15 Years of <i>Small</i>: Research Trends in Nanosafety. Small, 2020, 16, e2000980. 38 5.2 37 Glucose-responsive cascaded nanocatalytic reactor with self-modulation of the tumor 6.4 56 microenvironment for enhanced chemo-catalytic therapy. Materials Horizons, 2020, 7, 1834-1844. Grapheneâ€Based Smart Platforms for Combined Cancer Therapy. Advanced Materials, 2019, 31, e1800662. 40 11.1 233 The pharmaceutical multi-activity of metallofullerenol invigorates cancer therapy. Nanoscale, 2019, 11, 2.8 16 14528-14539. A Novel Drug Design Strategy: An Inspiration from Encaging Tumor by Metallofullerenol 42 1.7 8 Gd@C82(OH)22. Molecules, 2019, 24, 2387. Nanomedicineâ€Based Immunotherapy for the Treatment of Cancer Metastasis. Advanced Materials, 2019, 11.1 120 31, e1904156. Emerging Delivery Strategies of Carbon Monoxide for Therapeutic Applications: from CO Gas to CO 44 5.2 79 Releasing Nanomaterials. Small, 2019, 15, e1904382. Clinical Nanomaterials: A Safeâ€byâ€Design Strategy towards Safer Nanomaterials in Nanomedicines (Adv.) Tj ETQq1 1 0.784314 Simultaneous enzyme mimicking and chemical reduction mechanisms for nanoceria as a bio-antioxidant: a catalytic model bridging computations and experiments for nanozymes. Nanoscale, 2.8 100 46 2019, 11, 13289-13299. Strategies based on metal-based nanoparticles for hypoxic-tumor radiotherapy. Chemical Science, 2019, 3.7 10, 6932-6943. Recent advances of stimuli-responsive systems based on transition metal dichalcogenides for smart 48 2.9 29 cancer therapy. Journal of Materials Chemistry B, 2019, 7, 2588-2607. Enhanced radiosensitization of ternary Cu₃BiSe₃ nanoparticles by photo-induced hyperthermia in the second near-infrared biological window. Nanoscale, 2019, 11, 7157-7165. 2.8 23 Enhanced Generation of Non-Oxygen Dependent Free Radicals by Schottky-type Heterostructures of Auâ€"Bi₂S₃ Nanoparticles <i>via</i> X-ray-Induced Catalytic Reaction for 50 7.3 126 Radiosensitization. ACS Nano, 2019, 13, 5947-5958. Fabrication of CuNCs/LDHs Films with Excellent Luminescent Properties and Exploration of 1.8 Thermosensitivity. Industrial & amp; Engineering Chemistry Research, 2019, 58, 8009-8015. A Safeâ€byâ€Design Strategy towards Safer Nanomaterials in Nanomedicines. Advanced Materials, 2019, 31, 52 11.1 109 e1805391. Progress and Prospects of Graphdiyneâ€Based Materials in Biomedical Applications. Advanced Materials, 11.1 124 2019, 31, e18043⁸⁶. Tumor Microenvironment-Responsive Cu₂(OH)PO₄ Nanocrystals for Selective 54 and Controllable Radiosentization via the X-ray-Triggered Fenton-like Reaction. Nano Letters, 2019, 19, 4.5 142

LIANG YAN

1749-1757.

#	Article	IF	CITATIONS
55	Efficient Near Infrared Light Triggered Nitric Oxide Release Nanocomposites for Sensitizing Mild Photothermal Therapy. Advanced Science, 2019, 6, 1801122.	5.6	169
56	Translocation, biotransformation-related degradation, and toxicity assessment of polyvinylpyrrolidone-modified 2H-phase nano-MoS ₂ . Nanoscale, 2019, 11, 4767-4780.	2.8	47
57	3D halos assembled from Fe ₃ O ₄ /Au NPs with enhanced catalytic and optical properties. Nanoscale, 2019, 11, 20968-20976.	2.8	14
58	Emerging Strategies of Nanomaterialâ€Mediated Tumor Radiosensitization. Advanced Materials, 2019, 31, e1802244.	11.1	244
59	Generalized Preparation of Two-Dimensional Quasi-nanosheets via Self-assembly of Nanoparticles. Journal of the American Chemical Society, 2019, 141, 1725-1734.	6.6	29
60	Tumor microenvironment-manipulated radiocatalytic sensitizer based on bismuth heteropolytungstate for radiotherapy enhancement. Biomaterials, 2019, 189, 11-22.	5.7	132
61	Nanoparticle Ligand Exchange and Its Effects at the Nanoparticle–Cell Membrane Interface. Nano Letters, 2019, 19, 8-18.	4.5	84
62	Photoluminescence enhancement of silver nanoclusters assembled on the layered double hydroxides and their application to guanine detection. Talanta, 2019, 193, 161-167.	2.9	14
63	Graphdiyne Nanoparticles with High Free Radical Scavenging Activity for Radiation Protection. ACS Applied Materials & Interfaces, 2019, 11, 2579-2590.	4.0	115
64	Hydrotalcite monolayer toward high performance synergistic dual-modal imaging and cancer therapy. Biomaterials, 2018, 165, 14-24.	5.7	39
65	Graphdiyne Nanosheet-Based Drug Delivery Platform for Photothermal/Chemotherapy Combination Treatment of Cancer. ACS Applied Materials & Interfaces, 2018, 10, 8436-8442.	4.0	130
66	A DNA nanorobot functions as a cancer therapeutic in response to a molecular trigger in vivo. Nature Biotechnology, 2018, 36, 258-264.	9.4	1,066
67	Cu ₂ (OH)PO ₄ /reduced graphene oxide nanocomposites for enhanced photocatalytic degradation of 2,4-dichlorophenol under infrared light irradiation. RSC Advances, 2018, 8, 3611-3618.	1.7	18
68	Peroxidase-like activity of MoS ₂ nanoflakes with different modifications and their application for H ₂ O ₂ and glucose detection. Journal of Materials Chemistry B, 2018, 6, 487-498.	2.9	130
69	Intelligent MoS ₂ Nanotheranostic for Targeted and Enzyme-/pH-/NIR-Responsive Drug Delivery To Overcome Cancer Chemotherapy Resistance Guided by PET Imaging. ACS Applied Materials & Interfaces, 2018, 10, 4271-4284.	4.0	137
70	Molecular mechanism of Gd@C 82 (OH) 22 increasing collagen expression: Implication for encaging tumor. Biomaterials, 2018, 152, 24-36.	5.7	26
71	Biodegradable MoO _x nanoparticles with efficient near-infrared photothermal and photodynamic synergetic cancer therapy at the second biological window. Nanoscale, 2018, 10, 1517-1531.	2.8	144
72	Quantification of Nanomaterial/Nanomedicine Trafficking in Vivo. Analytical Chemistry, 2018, 90, 589-614.	3.2	85

#	Article	IF	CITATIONS
73	Fabrication of dual-stimuli responsive films assembled by flavin mononucleotide and layered double hydroxides. Chemical Communications, 2018, 54, 12590-12593.	2.2	5
74	Precise nanomedicine for intelligent therapy of cancer. Science China Chemistry, 2018, 61, 1503-1552.	4.2	336
75	Functionalized MoS ₂ Nanovehicle with Nearâ€Infrared Laserâ€Mediated Nitric Oxide Release and Photothermal Activities for Advanced Bacteriaâ€Infected Wound Therapy. Small, 2018, 14, e1802290.	5.2	259
76	Free-Floating 2D Nanosheets with a Superlattice Assembled from Fe3O4 Nanoparticles for Peroxidase-Mimicking Activity. ACS Applied Nano Materials, 2018, 1, 5389-5395.	2.4	9
77	Xâ€Rayâ€Controlled Generation of Peroxynitrite Based on Nanosized LiLuF ₄ :Ce ³⁺ Scintillators and their Applications for Radiosensitization. Advanced Materials, 2018, 30, e1804046.	11.1	138
78	Harnessing Tumor Microenvironment for Nanoparticleâ€Mediated Radiotherapy. Advanced Therapeutics, 2018, 1, 1800050.	1.6	33
79	Application of Multifunctional Nanomaterials in Radioprotection of Healthy Tissues. Advanced Healthcare Materials, 2018, 7, e1800421.	3.9	52
80	Gd@C82(OH)22 harnesses inflammatory regeneration for osteogenesis of mesenchymal stem cells through JNK/STAT3 signaling pathway. Journal of Materials Chemistry B, 2018, 6, 5802-5811.	2.9	12
81	Hyaluronic acid modified MPEG- <i>b</i> -PAE block copolymer aqueous micelles for efficient ophthalmic drug delivery of hydrophobic genistein. Drug Delivery, 2018, 25, 1258-1265.	2.5	37
82	Investigating oxidation state-induced toxicity of PEGylated graphene oxide in ocular tissue using gene expression profiles. Nanotoxicology, 2018, 12, 819-835.	1.6	28
83	Biodistribution, excretion, and toxicity of polyethyleneimine modified NaYF ₄ :Yb,Er upconversion nanoparticles in mice via different administration routes. Nanoscale, 2017, 9, 4497-4507.	2.8	61
84	Two-dimensional transition metal dichalcogenide nanomaterials for combination cancer therapy. Journal of Materials Chemistry B, 2017, 5, 1873-1895.	2.9	112
85	Protein-directed synthesis of Bi ₂ S ₃ nanoparticles as an efficient contrast agent for visualizing the gastrointestinal tract. RSC Advances, 2017, 7, 17505-17513.	1.7	15
86	Design of TPGS-functionalized Cu ₃ BiS ₃ nanocrystals with strong absorption in the second near-infrared window for radiation therapy enhancement. Nanoscale, 2017, 9, 8229-8239.	2.8	69
87	Chiral Surface of Nanoparticles Determines the Orientation of Adsorbed Transferrin and Its Interaction with Receptors. ACS Nano, 2017, 11, 4606-4616.	7.3	125
88	Polyoxometalate-Based Radiosensitization Platform for Treating Hypoxic Tumors by Attenuating Radioresistance and Enhancing Radiation Response. ACS Nano, 2017, 11, 7164-7176.	7.3	168
89	MoS ₂ -Nanosheet-Assisted Coordination of Metal Ions with Porphyrin for Rapid Detection and Removal of Cadmium Ions in Aqueous Media. ACS Applied Materials & Interfaces, 2017, 9, 21362-21370.	4.0	54
90	Therapeutic Nanoparticles Based on Curcumin and Bamboo Charcoal Nanoparticles for Chemo-Photothermal Synergistic Treatment of Cancer and Radioprotection of Normal Cells. ACS Applied Materials & Interfaces, 2017, 9, 14281-14291.	4.0	72

#	Article	IF	CITATIONS
91	Diverse Applications of Nanomedicine. ACS Nano, 2017, 11, 2313-2381.	7.3	976
92	Au Nanoclusters and Photosensitizer Dual Loaded Spatiotemporal Controllable Liposomal Nanocomposites Enhance Tumor Photodynamic Therapy Effect by Inhibiting Thioredoxin Reductase. Advanced Healthcare Materials, 2017, 6, 1601453.	3.9	30
93	Functional tumor imaging based on inorganic nanomaterials. Science China Chemistry, 2017, 60, 1425-1438.	4.2	17
94	Synthesis of BSAâ€Coated BiOI@Bi ₂ S ₃ Semiconductor Heterojunction Nanoparticles and Their Applications for Radio/Photodynamic/Photothermal Synergistic Therapy of Tumor. Advanced Materials, 2017, 29, 1704136.	11.1	257
95	Elemental Bismuth–Graphene Heterostructures for Photocatalysis from Ultraviolet to Infrared Light. ACS Catalysis, 2017, 7, 7043-7050.	5.5	65
96	Photothermal Effect Enhanced Cascade-Targeting Strategy for Improved Pancreatic Cancer Therapy by Gold Nanoshell@Mesoporous Silica Nanorod. ACS Nano, 2017, 11, 8103-8113.	7.3	135
97	Poly(Vinylpyrollidone)―and Selenocysteineâ€Modified Bi ₂ Se ₃ Nanoparticles Enhance Radiotherapy Efficacy in Tumors and Promote Radioprotection in Normal Tissues. Advanced Materials, 2017, 29, 1701268.	11.1	171
98	Metallofullerenol Inhibits Cellular Iron Uptake by Inducing Transferrin Tetramerization. Chemistry - an Asian Journal, 2017, 12, 2646-2651.	1.7	8
99	Ultrasmall Superparamagnetic Iron Oxide Nanoparticle for <i>T</i> ₂ -Weighted Magnetic Resonance Imaging. ACS Applied Materials & Interfaces, 2017, 9, 28959-28966.	4.0	61
100	Design, Synthesis, and Surface Modification of Materials Based on Transitionâ€Metal Dichalcogenides for Biomedical Applications. Small Methods, 2017, 1, 1700220.	4.6	86
101	Evaluation of the toxicity of graphene oxide exposure to the eye. Nanotoxicology, 2016, 10, 1329-1340.	1.6	62
102	Mesoporous Bamboo Charcoal Nanoparticles as a New Nearâ€Infrared Responsive Drug Carrier for Imagingâ€Guided Chemotherapy/Photothermal Synergistic Therapy of Tumor. Advanced Healthcare Materials, 2016, 5, 1627-1637.	3.9	34
103	<l>ln Vivo</l> Toxicity Evaluation of Graphene Oxide in <l>Drosophila Melanogaster</l> After Oral Administration. Journal of Nanoscience and Nanotechnology, 2016, 16, 7472-7478.	0.9	5
104	Transformable Peptide Nanocarriers for Expeditious Drug Release and Effective Cancer Therapy via Cancerâ€Associated Fibroblast Activation. Angewandte Chemie - International Edition, 2016, 55, 1050-1055.	7.2	153
105	Nitric oxide-generating <scp>l</scp> -cysteine-grafted graphene film as a blood-contacting biomaterial. Biomaterials Science, 2016, 4, 938-942.	2.6	17
106	The polyvinylpyrrolidone functionalized rGO/Bi ₂ S ₃ nanocomposite as a near-infrared light-responsive nanovehicle for chemo-photothermal therapy of cancer. Nanoscale, 2016, 8, 11531-11542.	2.8	71
107	Gdâ€Hybridized Plasmonic Auâ€Nanocomposites Enhanced Tumorâ€Interior Drug Permeability in Multimodal Imagingâ€Guided Therapy. Advanced Materials, 2016, 28, 8950-8958.	11.1	138
108	Functionalized Nano-MoS ₂ with Peroxidase Catalytic and Near-Infrared Photothermal Activities for Safe and Synergetic Wound Antibacterial Applications. ACS Nano, 2016, 10, 11000-11011.	7.3	812

#	Article	IF	CITATIONS
109	Co-delivery of doxorubicin and quercetin via mPEG–PLGA copolymer assembly for synergistic anti-tumor efficacy and reducing cardio-toxicity. Science Bulletin, 2016, 61, 1689-1698.	4.3	32
110	Gadolinium polytungstate nanoclusters: a new theranostic with ultrasmall size and versatile properties for dual-modal MR/CT imaging and photothermal therapy/radiotherapy of cancer. NPG Asia Materials, 2016, 8, e273-e273.	3.8	75
111	Proteinâ€Nanoreactorâ€Assisted Synthesis of Semiconductor Nanocrystals for Efficient Cancer Theranostics. Advanced Materials, 2016, 28, 5923-5930.	11.1	175
112	Aspect ratios of gold nanoshell capsules mediated melanoma ablation by synergistic photothermal therapy and chemotherapy. Nanomedicine: Nanotechnology, Biology, and Medicine, 2016, 12, 439-448.	1.7	41
113	One-pot synthesis of PEGylated plasmonic MoO3–x hollow nanospheres for photoacoustic imaging guided chemo-photothermal combinational therapy of cancer. Biomaterials, 2016, 76, 11-24.	5.7	171
114	Recent Advances in Upconversion Nanoparticlesâ€Based Multifunctional Nanocomposites for Combined Cancer Therapy. Advanced Materials, 2015, 27, 7692-7712.	11.1	243
115	Phytotoxicity, Translocation, and Biotransformation of NaYF ₄ Upconversion Nanoparticles in a Soybean Plant. Small, 2015, 11, 4774-4784.	5.2	49
116	Silver nanoparticles activate endoplasmic reticulum stress signaling pathway in cell and mouse models: The role in toxicity evaluation. Biomaterials, 2015, 61, 307-315.	5.7	121
117	Smart MoS ₂ /Fe ₃ O ₄ Nanotheranostic for Magnetically Targeted Photothermal Therapy Guided by Magnetic Resonance/Photoacoustic Imaging. Theranostics, 2015, 5, 931-945.	4.6	234
118	Use of Synchrotron Radiation-Analytical Techniques To Reveal Chemical Origin of Silver-Nanoparticle Cytotoxicity. ACS Nano, 2015, 9, 6532-6547.	7.3	246
119	Near-infrared light remote-controlled intracellular anti-cancer drug delivery using thermo/pH sensitive nanovehicle. Acta Biomaterialia, 2015, 17, 201-209.	4.1	145
120	Bismuth Sulfide Nanorods as a Precision Nanomedicine for <i>in Vivo</i> Multimodal Imaging-Guided Photothermal Therapy of Tumor. ACS Nano, 2015, 9, 696-707.	7.3	503
121	Gd-metallofullerenol nanomaterial as non-toxic breast cancer stem cell-specific inhibitor. Nature Communications, 2015, 6, 5988.	5.8	164
122	Towards understanding of nanoparticle–protein corona. Archives of Toxicology, 2015, 89, 519-539.	1.9	135
123	Nanosurface chemistry and dose govern the bioaccumulation and toxicity of carbon nanotubes, metal nanomaterials and quantum dots in vivo. Science Bulletin, 2015, 60, 3-20.	4.3	96
124	Gd–Metallofullerenol Nanomaterial Suppresses Pancreatic Cancer Metastasis by Inhibiting the Interaction of Histone Deacetylase 1 and Metastasis-Associated Protein 1. ACS Nano, 2015, 9, 6826-6836.	7.3	64
125	Silica-coated bismuth sulfide nanorods as multimodal contrast agents for a non-invasive visualization of the gastrointestinal tract. Nanoscale, 2015, 7, 12581-12591.	2.8	60
126	Deciphering the underlying mechanisms of oxidation-state dependent cytotoxicity of graphene oxide on mammalian cells. Toxicology Letters, 2015, 237, 61-71.	0.4	100

#	Article	IF	CITATIONS
127	Ultrasmall [⁶⁴ Cu]Cu Nanoclusters for Targeting Orthotopic Lung Tumors Using Accurate Positron Emission Tomography Imaging. ACS Nano, 2015, 9, 4976-4986.	7.3	108
128	Enhanced Multifunctional Properties of Graphene Nanocomposites with Nacre‣ike Structures. Advanced Engineering Materials, 2015, 17, 523-531.	1.6	15
129	Controllable Generation of Nitric Oxide by Nearâ€Infraredâ€6ensitized Upconversion Nanoparticles for Tumor Therapy. Advanced Functional Materials, 2015, 25, 3049-3056.	7.8	194
130	Synchrotron radiation techniques for nanotoxicology. Nanomedicine: Nanotechnology, Biology, and Medicine, 2015, 11, 1531-1549.	1.7	29
131	Tungsten Sulfide Quantum Dots as Multifunctional Nanotheranostics for <i>In Vivo</i> Dual-Modal Image-Guided Photothermal/Radiotherapy Synergistic Therapy. ACS Nano, 2015, 9, 12451-12463.	7.3	388
132	Protein Corona Influences Cellular Uptake of Gold Nanoparticles by Phagocytic and Nonphagocytic Cells in a Size-Dependent Manner. ACS Applied Materials & Interfaces, 2015, 7, 20568-20575.	4.0	243
133	Quantifying the distribution of ceria nanoparticles in cucumber roots: the influence of labeling. RSC Advances, 2015, 5, 4554-4560.	1.7	18
134	Parallel Comparative Studies on Mouse Toxicity of Oxide Nanoparticle- and Gadolinium-Based T1 MRI Contrast Agents. ACS Nano, 2015, 9, 12425-12435.	7.3	145
135	TPGS-stabilized NaYbF4:Er upconversion nanoparticles for dual-modal fluorescent/CT imaging and anticancer drug delivery to overcome multi-drug resistance. Biomaterials, 2015, 40, 107-116.	5.7	172
136	Multifunctional Rb <i>_x</i> WO ₃ Nanorods for Simultaneous Combined Chemoâ€photothermal Therapy and Photoacoustic/CT Imaging. Small, 2014, 10, 4160-4170.	5.2	86
137	Polyhydroxylated Metallofullerenols Stimulate ILâ€1β Secretion of Macrophage through TLRs/MyD88/NFâ€₽® Pathway and NLRP ₃ Inflammasome Activation. Small, 2014, 10, 2362-2372.	5.2	96
138	Novel Insights into Combating Cancer Chemotherapy Resistance Using a Plasmonic Nanocarrier: Enhancing Drug Sensitiveness and Accumulation Simultaneously with Localized Mild Photothermal Stimulus of Femtosecond Pulsed Laser. Advanced Functional Materials, 2014, 24, 4229-4239.	7.8	130
139	Regulation on mechanical properties of collagen: Enhanced bioactivities of metallofullerol. Nanomedicine: Nanotechnology, Biology, and Medicine, 2014, 10, 783-793.	1.7	12
140	A magnetic graphene hybrid functionalized with beta-cyclodextrins for fast and efficient removal of organic dyes. Journal of Materials Chemistry A, 2014, 2, 12296.	5.2	113
141	Biocompatible and flexible graphene oxide/upconversion nanoparticle hybrid film for optical pH sensing. Physical Chemistry Chemical Physics, 2014, 16, 1576-1582.	1.3	57
142	Design of multifunctional alkali ion doped CaF2 upconversion nanoparticles for simultaneous bioimaging and therapy. Dalton Transactions, 2014, 43, 3861.	1.6	36
143	Elimination of Photon Quenching by a Transition Layer to Fabricate a Quenchingâ€5hield Sandwich Structure for 800 nm Excited Upconversion Luminescence of Nd ³⁺ â€5ensitized Nanoparticles. Advanced Materials, 2014, 26, 2831-2837.	11.1	405
144	On-demand generation of singlet oxygen from a smart graphene complex for the photodynamic treatment of cancer cells. Biomaterials Science, 2014, 2, 1412-1418.	2.6	26

#	Article	IF	CITATIONS
145	A simple and efficient synthetic route for preparation of NaYF ₄ upconversion nanoparticles by thermo-decomposition of rare-earth oleates. CrystEngComm, 2014, 16, 5650-5661.	1.3	35
146	Energy metabolism analysis reveals the mechanism of inhibition of breast cancer cell metastasis by PEG-modified graphene oxide nanosheets. Biomaterials, 2014, 35, 9833-9843.	5.7	99
147	WS ₂ nanosheet as a new photosensitizer carrier for combined photodynamic and photothermal therapy of cancer cells. Nanoscale, 2014, 6, 10394-10403.	2.8	301
148	Near Infrared Laser-Induced Targeted Cancer Therapy Using Thermoresponsive Polymer Encapsulated Gold Nanorods. Journal of the American Chemical Society, 2014, 136, 7317-7326.	6.6	569
149	High-Throughput Synthesis of Single-Layer MoS ₂ Nanosheets as a Near-Infrared Photothermal-Triggered Drug Delivery for Effective Cancer Therapy. ACS Nano, 2014, 8, 6922-6933.	7.3	813
150	Oneâ€Pot Templateâ€Free Synthesis of NaYF ₄ Upconversion Hollow Nanospheres for Bioimaging and Drug Delivery. Chemistry - an Asian Journal, 2014, 9, 1655-1662.	1.7	22
151	Recent Advances in Design and Fabrication of Upconversion Nanoparticles and Their Safe Theranostic Applications. Advanced Materials, 2013, 25, 3758-3779.	11.1	437
152	Advanced nuclear analytical and related techniques for the growing challenges in nanotoxicology. Chemical Society Reviews, 2013, 42, 8266.	18.7	104
153	Chemical Mechanisms of the Toxicological Properties of Nanomaterials: Generation of Intracellular Reactive Oxygen Species. Chemistry - an Asian Journal, 2013, 8, 2342-2353.	1.7	79
154	A new near infrared photosensitizing nanoplatform containing blue-emitting up-conversion nanoparticles and hypocrellin A for photodynamic therapy of cancer cells. Nanoscale, 2013, 5, 11910.	2.8	85
155	Biological characterizations of [Cd@C82(OH)22] <i>n</i> nanoparticles as fullerene derivatives for cancer therapy. Integrative Biology (United Kingdom), 2013, 5, 43-47.	0.6	76
156	Interactions Between Proteins and Carbonâ€Based Nanoparticles: Exploring the Origin of Nanotoxicity at the Molecular Level. Small, 2013, 9, 1546-1556.	5.2	132
157	Physicochemical Properties Determine Nanomaterial Cellular Uptake, Transport, and Fate. Accounts of Chemical Research, 2013, 46, 622-631.	7.6	627
158	Revealing the Binding Structure of the Protein Corona on Gold Nanorods Using Synchrotron Radiation-Based Techniques: Understanding the Reduced Damage in Cell Membranes. Journal of the American Chemical Society, 2013, 135, 17359-17368.	6.6	239
159	Metabolism of Nanomaterials <i>in Vivo</i> : Blood Circulation and Organ Clearance. Accounts of Chemical Research, 2013, 46, 761-769.	7.6	424
160	Understanding the Toxicity of Carbon Nanotubes. Accounts of Chemical Research, 2013, 46, 702-713.	7.6	623
161	Redâ€Emitting Upconverting Nanoparticles for Photodynamic Therapy in Cancer Cells Under Nearâ€Infrared Excitation. Small, 2013, 9, 1929-1938.	5.2	174
162	The use of polyethylenimine-modified graphene oxide as a nanocarrier for transferring hydrophobic nanocrystals into water to produce water-dispersible hybrids for use in drug delivery. Carbon, 2013, 57, 120-129.	5.4	92

#	Article	IF	CITATIONS
163	Filling Knowledge Gaps that Distinguish the Safety Profiles of Nano versus Bulk Materials. Small, 2013, 9, 1426-1427.	5.2	10
164	Temporal Techniques: Dynamic Tracking of Nanomaterials in Live Cells. Small, 2013, 9, 1585-1594.	5.2	15
165	Interfacing Engineered Nanoparticles with Biological Systems: Anticipating Adverse Nano–Bio Interactions. Small, 2013, 9, 1573-1584.	5.2	176
166	Upconversion: Redâ€Emitting Upconverting Nanoparticles for Photodynamic Therapy in Cancer Cells Under Nearâ€Infrared Excitation (Small 11/2013). Small, 2013, 9, 1928-1928.	5.2	8
167	Short Multiwall Carbon Nanotubes Promote Neuronal Differentiation of PC12 Cells via Upâ€Regulation of the Neurotrophin Signaling Pathway. Small, 2013, 9, 1786-1798.	5.2	52
168	Characterization and Preliminary Toxicity Assay of Nanoâ€Titanium Dioxide Additive in Sugar oated Chewing Gum. Small, 2013, 9, 1765-1774.	5.2	209
169	Multiwall Carbon Nanotubes Mediate Macrophage Activation and Promote Pulmonary Fibrosis Through TGFâ€Î²/Smad Signaling Pathway. Small, 2013, 9, 3799-3811.	5.2	121
170	Molecular mechanism of pancreatic tumor metastasis inhibition by Gd@C ₈₂ (OH) ₂₂ and its implication for de novo design of nanomedicine. Proceedings of the National Academy of Sciences of the United States of America, 2012, 109, 15431-15436.	3.3	200
171	Lanthanide-doped GdVO4 upconversion nanophosphors with tunable emissions and their applications for biomedical imaging. Journal of Materials Chemistry, 2012, 22, 6974.	6.7	124
172	Controllable synthesis of Gd2O(CO3)2·H2O@silica–FITC nanoparticles with size-dependent optical and magnetic resonance imaging properties. New Journal of Chemistry, 2012, 36, 2599.	1.4	15
173	TWEEN coated NaYF4:Yb,Er/NaYF4 core/shell upconversion nanoparticles for bioimaging and drug delivery. RSC Advances, 2012, 2, 7037.	1.7	98
174	Comparative toxicity of nanoparticulate/bulk Yb ₂ O ₃ and YbCl ₃ to cucumber (<i>Cucumis sativus</i>). Environmental Science & Technology, 2012, 46, 1834-1841.	4.6	153
175	Effects of gestational age and surface modification on materno-fetal transfer of nanoparticles in murine pregnancy. Scientific Reports, 2012, 2, 847.	1.6	104
176	Size-tunable synthesis of lanthanide-doped Gd ₂ O ₃ nanoparticles and their applications for optical and magnetic resonance imaging. Journal of Materials Chemistry, 2012, 22, 966-974.	6.7	165
177	Chemistry and physics of a single atomic layer: strategies and challenges for functionalization of graphene and graphene-based materials. Chemical Society Reviews, 2012, 41, 97-114.	18.7	487
178	Lanthanide ion-doped GdPO4 nanorods with dual-modal bio-optical and magnetic resonance imaging properties. Nanoscale, 2012, 4, 3754.	2.8	113
179	Enhanced Red Emission from GdF ₃ :Yb ³⁺ ,Er ³⁺ Upconversion Nanocrystals by Li ⁺ Doping and Their Application for Bioimaging. Chemistry - A European Journal, 2012, 18, 9239-9245.	1.7	166
180	Gadolinium metallofullerenol nanoparticles inhibit cancer metastasis through matrix metalloproteinase inhibition: imprisoning instead of poisoning cancer cells. Nanomedicine: Nanotechnology, Biology, and Medicine, 2012, 8, 136-146.	1.7	101

#	Article	IF	CITATIONS
181	Mn ²⁺ Dopantâ€Controlled Synthesis of NaYF ₄ :Yb/Er Upconversion Nanoparticles for in vivo Imaging and Drug Delivery. Advanced Materials, 2012, 24, 1226-1231.	11.1	758
182	Binding of blood proteins to carbon nanotubes reduces cytotoxicity. Proceedings of the National Academy of Sciences of the United States of America, 2011, 108, 16968-16973.	3.3	839
183	Regioselectivity control of graphene functionalization by ripples. Physical Chemistry Chemical Physics, 2011, 13, 19449.	1.3	46
184	Controlling Assembly of Paired Gold Clusters within Apoferritin Nanoreactor for in Vivo Kidney Targeting and Biomedical Imaging. Journal of the American Chemical Society, 2011, 133, 8617-8624.	6.6	258
185	Full Assessment of Fate and Physiological Behavior of Quantum Dots Utilizing <i>Caenorhabditis elegans</i> as a Model Organism. Nano Letters, 2011, 11, 3174-3183.	4.5	212
186	Biosafety assessment of Gd@C82(OH)22 nanoparticles on Caenorhabditis elegans. Nanoscale, 2011, 3, 2636.	2.8	46
187	Facile Fabrication of Rare-Earth-Doped Gd ₂ O ₃ Hollow Spheres with Upconversion Luminescence, Magnetic Resonance, and Drug Delivery Properties. Journal of Physical Chemistry C, 2011, 115, 23790-23796.	1.5	170
188	Low-toxic and safe nanomaterials by surface-chemical design, carbon nanotubes, fullerenes, metallofullerenes, and graphenes. Nanoscale, 2011, 3, 362-382.	2.8	264
189	Epigenetic modulation of human breast cancer by metallofullerenol nanoparticles: in vivo treatment and in vitro analysis. Nanoscale, 2011, 3, 4713.	2.8	30
190	Cellular Uptake, Intracellular Trafficking, and Cytotoxicity of Nanomaterials. Small, 2011, 7, 1322-1337.	5.2	975
191	Chirality of Glutathione Surface Coating Affects the Cytotoxicity of Quantum Dots. Angewandte Chemie - International Edition, 2011, 50, 5860-5864.	7.2	210
192	Lung deposition and extrapulmonary translocation of nano-ceria after intratracheal instillation. Nanotechnology, 2010, 21, 285103.	1.3	137
193	Chemistry of carbon nanotubes in biomedical applications. Journal of Materials Chemistry, 2010, 20, 1036-1052.	6.7	235
194	[Gd@C ₈₂ (OH) ₂₂] _{<i>n</i>} Nanoparticles Induce Dendritic Cell Maturation and Activate Th1 Immune Responses. ACS Nano, 2010, 4, 1178-1186.	7.3	131
195	Potent Angiogenesis Inhibition by the Particulate Form of Fullerene Derivatives. ACS Nano, 2010, 4, 2773-2783.	7.3	148
196	Ecotoxicological assessment of lanthanum with Caenorhabditis elegans in liquid medium. Metallomics, 2010, 2, 806.	1.0	42
197	Metallofullerene nanoparticles circumvent tumor resistance to cisplatin by reactivating endocytosis. Proceedings of the National Academy of Sciences of the United States of America, 2010, 107, 7449-7454.	3.3	233
198	The effect of Gd@C82(OH)22 nanoparticles on the release of Th1/Th2 cytokines and induction of TNF-α mediated cellular immunity. Biomaterials, 2009, 30, 3934-3945.	5.7	177

#	Article	IF	CITATIONS
199	The scavenging of reactive oxygen species and the potential for cell protection by functionalized fullerene materials. Biomaterials, 2009, 30, 611-621.	5.7	388
200	Bio-distribution and metabolic paths of silica coated CdSeS quantum dots. Toxicology and Applied Pharmacology, 2008, 230, 364-371.	1.3	145
201	Potential neurological lesion after nasal instillation of TiO2 nanoparticles in the anatase and rutile crystal phases. Toxicology Letters, 2008, 183, 72-80.	0.4	310
202	Mapping technique for biodistribution of elements in a model organism, Caenorhabditis elegans, after exposure to copper nanoparticles with microbeam synchrotron radiation X-ray fluorescence. Journal of Analytical Atomic Spectrometry, 2008, 23, 1121.	1.6	75
203	Inhibition of Tumor Growth by Endohedral Metallofullerenol Nanoparticles Optimized as Reactive Oxygen Species Scavenger. Molecular Pharmacology, 2008, 74, 1132-1140.	1.0	117
204	Modulation of Structural and Electronic Properties of Fullerene and Metallofullerenes by Surface Chemical Modifications. Journal of Nanoscience and Nanotechnology, 2007, 7, 1085-1101.	0.9	26
205	Acute toxicity and biodistribution of different sized titanium dioxide particles in mice after oral administration. Toxicology Letters, 2007, 168, 176-185.	0.4	973
206	Ytterbium and trace element distribution in brain and organic tissues of offspring rats after prenatal and postnatal exposure to ytterbium. Biological Trace Element Research, 2007, 117, 89-104.	1.9	25
207	Study of multihydroxylated processes of Gd@C82 by ICP-MASS. Journal of Radioanalytical and Nuclear Chemistry, 2007, 272, 537-540.	0.7	9
208	Study of rare earth encapsulated carbon nanomolecules for biomedical uses. Journal of Alloys and Compounds, 2006, 408-412, 400-404.	2.8	28
209	Antioxidative function and biodistribution of [Gd@C82(OH)22]n nanoparticles in tumor-bearing mice. Biochemical Pharmacology, 2006, 71, 872-881.	2.0	152
210	Cytotoxicity of Carbon Nanomaterials:Â Single-Wall Nanotube, Multi-Wall Nanotube, and Fullerene. Environmental Science & Technology, 2005, 39, 1378-1383.	4.6	1,307
211	Multihydroxylated [Gd@C82(OH)22]nNanoparticles:Â Antineoplastic Activity of High Efficiency and Low Toxicity. Nano Letters, 2005, 5, 2050-2057.	4.5	281
212	Tuning Electronic Properties of Metallic Atom in Bondage to a Nanospace. Journal of Physical Chemistry B, 2005, 109, 8779-8785.	1.2	38
213	Biodistribution of Carbon Single-Wall Carbon Nanotubes in Mice. Journal of Nanoscience and Nanotechnology, 2004, 4, 1019-1024.	0.9	355
214	Influences of Structural Properties on Stability of Fullerenols. Journal of Physical Chemistry B, 2004, 108, 11473-11479.	1.2	139
215	The effect of fullerenols on streptozotocin-induced diabetic rats. Fullerenes Nanotubes and Carbon Nanostructures, 0, , 1-14.	1.0	0